Brain Behav Immun. Author manuscript; available in PMC 2016 September 13.

Published in final edited form as:

Brain Behav Immun. 2007 July ; 21(5): 624–633. doi:10.1016/j.bbi.2006.10.017.

Stereological and somatotopic analysis of the spinal microglial response to peripheral nerve injury

Simon Beggs[a,b,*] and **Michael W. Salter**[a]

[a]University of Toronto Centre for the Study of Pain, The Program in Neurosciences and Mental Health, Hospital for Sick Children, Toronto, Ont., Canada

[b]Faculty of Dentistry, University of Toronto, Ont., Canada

Abstract

The involvement of glia, and glia-neuronal signalling in enhancing nociceptive transmission has become an area of intense scientific interest. In particular, a role has emerged for activated microglia in the development and maintenance of neuropathic pain following peripheral nerve injury. Following activation, spinal microglia proliferate and release many substances which are capable of modulating neuronal excitability within the spinal cord. Here, we the investigated the response of spinal microglia to a unilateral spared nerve injury (SNI) in terms of the quantitative increase in cell number and the spatial distribution of the increase. Design-based stereological techniques were combined with iba-1 immunohistochemistry to estimate the total number of microglia in the spinal dorsal horn in naïve and peripheral nerve-injured adult rats. In addition, by mapping the central terminals of hindlimb nerves, the somatotopic distribution of the microglial response was mapped. Following SNI there was a marked increase in the number of spinal microglia: The total number of microglia (mean ± SD) in the dorsal horn sciatic territory of the naïve rat was estimated to be 28,591 ± 2715. Following SNI the number of microglia was 82,034 ± 8828. While the pattern of microglial activation generally followed somatotopic boundaries, with the majority of microglia within the territory occupied by peripherally axotomised primary afferents, some spread was seen into regions occupied by intact, ‘spared’ central projections of the sural nerve. This study provides a reproducible method of assaying spinal microglial dynamics following peripheral nerve injury both quantitatively and spatially.

Keywords

Microglia; Spinal cord; Stereology; Somatotopy; Pain

1. Introduction

Chronic neuropathic pain following peripheral nerve injury represents a major problem in health care and persists in often being refractory to conventional treatment (Scholz and Woolf, 2002; Tsuda et al., 2005). Multiple mechanisms have been proposed to underlie the long-term changes associated with pain states that persist long after any initial injury has

*Corresponding author. simon.beggs@utoronto.ca (S. Beggs).

healed. It is likely that considerable redundancy exists and that multiple mechanisms both in the peripheral and central nervous systems contribute to the maintenance of neuropathic pain. It is generally accepted that there is a considerable central component and that increased spinal neuronal excitability mediates, at least in part, the pathological pain state. In recent years much attention has been focused on the role of glial cells and in particular their interaction with first and second order neurons in the central nervous system through the release of cytokines, neurotrophic factors and other pro-inflammatory molecules as direct modulators of neuronal excitability. Microglia in particular have been implicated in this role.

The role of microglia as sensors of CNS damage is well described in many neuropathological conditions. It is becoming increasingly clear that their function goes beyond that of sensor and that they represent a key causative component of certain pathologies such as neuropathic pain. Peripheral nerve injury often results in a chronic pain conditions that have a strong central component. Recently it has been shown that microglia mediate this central response. PNI induces a marked microglial reaction in the dorsal horn of the spinal cord. Microglia respond with a stereotypical ‘activation’—their numbers swell through proliferation and infiltration and they change their morphology from the characteristic ramified ‘resting’ state to the more amoeboid ‘activated’ state, a process also associated with considerable change in gene expression (Perry, 1994; Kreutzberg, 1996; Stoll and Jander, 1999; Nakajima and Kohsaka, 2001). This ‘activation’ response has been reported in all experimental models of neuropathic pain involving peripheral nerve injury (Liu et al., 1995; Coyle, 1998; Colburn et al., 1999; Herzberg and Sagen, 2001; Tsuda et al., 2003; Zhang and De Koninck, 2006). In all cases the response is typified by a marked increase in the number of microglia in the ipsilateral dorsal horn of the spinal cord.

Activation of microglia is characterized by the production and secretion of proinflammatory cytokines and other mediators that could potentially contribute to the initiation and maintenance of pain hypersensitivity. Other proteins indicative of activation include members of the complement cascade; complement receptor 3 (CR3), Toll-like receptor 4 (TLR4), CD14, CD4 and major histocompatibility complex (MHC) class I and II. A correlation between an upregulation of many of these markers in the spinal cord and peripheral nerve injury has long been reported (Gehrmann et al., 1991; Streit et al., 1988; Eriksson et al., 1993; Liu et al., 1995). The coincident onset of pain behavior with increases in microglial activity has also been well documented (Colburn et al., 1997; Coyle, 1998; Colburn et al., 1999), but it is only recently that a causal role of microglial activation in nerve injury-induced pain behaviors has been established (Tsuda et al., 2003; Jin et al., 2003) and the key mediator released by microglia identified as BDNF (Coull et al., 2005).

There is a wealth of research detailing the production and secretion of many cytokines, chemokines and other proinflammatory mediators from microglia within the CNS following peripheral nerve injury (Wieseler-Frank et al., 2004; Tsuda et al., 2005; Moalem and Tracey, 2006) and many of these factors are also capable of contributing to the changes in second order neuronal excitability seen following nerve injury that underlie neuropathic pain behaviours (Watkins et al., 2001; Ji et al., 2003; Salter, 2005). The relative spatial distribution of injured peripheral nerve central terminals, microglial cells and second order dorsal horn cells within the spinal dorsal horn is, therefore, of key importance when

considering a signalling pathway that involves these three elements. The activation of spinal microglia involves the production and secretion of the many proinflammatory factors from a proliferating population. The concentration of these factors and by extension the effect on second order neurons and spinal excitability will be determined by both the amount of proliferation and the spatial location within the spinal cord. It is important, therefore, to take into consideration these two phenomena when examining the central microglial response to peripheral injury.

In contrast to other CNS areas, where considerable effort has been made to stereologically quantify the microglial response to a wide range of stimuli (Long et al., 1998; Ayoub and Salm, 2003; Wirenfeldt et al., 2003), few reports have attempted to quantify the microglial response to injury to peripheral sensory nerves (Eriksson et al., 1993; Melzer et al., 1997; Fu et al., 1999) and none has used design-based counting techniques. The use of immunoreactive profiles as a measure of cell density will likely introduce an inherent error due to the change in size of the microglial soma upon activation (Melzer et al., 1997). Other studies have described the somatotopic distribution of the central microglial reaction to peripheral nerve injury (Melzer et al., 1997), yet no reports have attempted to characterize the details or accuracy of this somatotopy within the spinal cord.

Here we use design-based stereological counting techniques to make accurate estimates of the number of microglia in the dorsal horn of the spinal cord following spared nerve injury. The optical fractionator technique (West et al., 1991, 1996) allows stereological principles to be used for counting tissue preparations that were previously unsuitable to such techniques. The advantages are that estimates of total cell number are unaffected by uniform tissue shrinkage, often a confounding factor in previous estimates. The fixation, cutting and mounting procedures necessary for optimal immunohistochemistry inevitably result in significant tissue shrinkage. For the optional fractionator, assuming that the immunostaining penetrates the full thickness of the tissue, and that the thickness of sections is measurable, these issues are overcome. Similarly, measurements of the volume or area of the tissue being investigated are also unnecessary, again an advantage when looking at a region of the CNS that changes both shape and area from section to section, such as the spinal cord dorsal horn. The optional fractionator relies on the cell type under investigation to be identifiable, as well as the anatomical boundaries within which those cells of interest lie. In essence the optional fractionator estimates the total number of cells by directly counting the number of those cells in a known fraction of the total volume of tissue of interest, in this case the grey matter of the lumbar dorsal horn.

2. Methods

2.1. Animals and surgery

A total of eight adult male Wistar rats (250–275 g) were used for this study. Animals were housed in pairs and maintained on a 12:12 h light–dark cycle with ad libitum access to food and water. All procedures were in accordance with the guidelines of the Canadian Council on Animal Care and approved by the Animal Care Committee of the Hospital for Sick Children.

The spared nerve injury (SNI) model of peripheral nerve injury was used as it has several advantages over other models (discussed later). Surgery was performed as described previously (Decosterd and Woolf, 2000). Briefly, rats were anaesthetized by iso-fluorane inhalation and the left sciatic nerve exposed under aseptic conditions. The distal trifurcation of the sciatic nerve was identified and the tibial and common peroneal branches ligated and cut, leaving the sural branch intact. The wound was sutured closed and the animals allowed to recover and returned to their housing.

In order for the central terminals of sciatic primary afferents to be identified, all eight animals were injected with the transganglionic tracer CTB-HRP (β-subunit of cholera toxin conjugated to HRP: List Labs). Eleven days following surgery the sciatic nerve was again exposed and 1 μl of 1% CTB conjugate injected into the transected nerve branches of the SNI animals or the entire sciatic nerve of the naïve group using a fine-tipped Hamilton microsyringe. Care was taken to just pierce the perineurium and allow the tracer to ‘wash over’ the nerve, so as to minimize any further damage to the sciatic nerve. Wounds were again closed and animals allowed to recover.

Three days later, all animals were perfused transcardially under urethane anaesthesia with 4% paraformaldehyde and the entire lumbar spinal cords removed, postfixed and cryoprotected overnight in 30% sucrose solution at 4 °C.

2.2. Tissue processing

Transverse sections of the lumbar spinal cord were cut at 50 μm using a microtome. A series of sections were collected free-floating for subsequent immunostaining and a further series mounted serially on slides for later somatotopic analysis.

2.3. Immunohistochemistry

Free-floating sections were washed in phosphate-buffered saline (PBS) and blocked in 10% normal donkey serum with 0.3% triton for 1 h. Sections were then incubated with combinations of the following antibodies: anti-rabbit iba-1 (1:2000, Dako, Denmark); anti-goat CTB (1:1000, List Labs). All sections were incubated at 4 °C for 48 h. Sections were washed in PBS (3 × 10 min) and incubated in fluorescently conjugated secondary antibodies; Cy3 donkey anti-goat, Cy5 donkey anti-rabbit (1:1000, Jackson) and FITC-conjugated IB4 (10 μg/ml, Sigma) for three hours at room temperature. Following a final wash in PBS (3 × 10 min), sections were mounted on saline coated slides (Sigma) allowed to air dry and coverslipped with Gelmount (Sigma).

2.4. Stereological analysis

The optional fractionator was used to estimate the total number of iba- 1 immunoreactive microglia in the lumbar dorsal horn. All sections were sectioned, stained and counted concurrently to reduce any variation in staining intensity. Pilot studies were used to determine the optimal number and spacing of sections. A uniform random systematic sampling pattern is vital to ensure accurate estimates of cell number: the first section was taken at random to fulfil the criteria for random sampling and further sections taken

systematically every 20th section through the lumbar cord giving a total of approximately 10 sections to be counted from each lumbar spinal cord.

All stereological analyses were carried out using a Leica DMIRE2 spinning disc confocal microscope equipped with an ASI motorized XY stage and Improvision Piezo focus drive. For the sampling of each section a grid was superimposed onto the spinal cord section with the step length between grid intersections 200 μm in both *x* and *y* planes. At each intersection the tissue was viewed under a 100× oil immersion objective and the field of view on the monitor used as the counting frame, with an area of 75 × 75 μm^2. The thickness of each section was determined before counting proceeded and a 20 μm optical dissector (*h*) used for counting to ensure adequate guard zones could be excluded on the upper and lower edges of the section (Fig. 2A) (for a 30 μm section the upper and lower guard zones were set at 5 μm). In each sampling frame, the *z*-axis was adjusted to account for the upper guard zone and iba-1 immunoreactive microglia were counted as each cell body came into view while focusing down through the 20 μm optical dissector. Any cells that intercepted the left or lower edges of the counting frame at any point throughout the extent of the cell body were not included.

The grey matter of the dorsal horn was chosen as the region within which total cell number would be counted. The difference in background staining intensity between grey and white matter in the dorsal horn allowed the two to be easily delineated.

2.5. Image acquisition and analysis

Images were acquired using Volocity software (Improvision). For the somatotopy images, Z-series were stacked and thresholds set for separate RGB channels using Photoshop (Adobe).

2.6. Estimate of total cell number

The total number of microglia (*N*) in a single lumbar dorsal horn was estimated using the methods of West et al. (1991):

$$N = \sum Q^{-} \cdot \frac{1}{\text{tsf}} \cdot \frac{1}{\text{asf}} \cdot \frac{1}{\text{ssf}}$$

where ΣQ^{-} is the total number of microglial cells counted, tsf is the thickness sampling fraction (*h*/*t*), asf is the area sampling fraction (counting frame area/step area) and ssf is the section sampling fraction (1/20).

Cell counts were statistically analysed using Student's *t*-test and a value of $p < 0.05$ was considered significant.

3. Results

3.1. Stereological counting of microglia in the dorsal horn

The principle of the optical fractionator technique is shown in Fig. 1a. The left panel is a schematic showing the grid used for placing the counting frames and the relationship in space of the counting frame to the section. Black squares are the positions of the counting

frames in each step area. The right panel represents a side elevation through the section and illustrates the use of guard zones and the 20 μm optical dissector. Cells were counted by manually focussing down through the optical dissector. For illustrative purposes, nine separate, adjacent z-series images are shown in Fig. 1b. Individual cells were counted as the cell body came into focus (shown by yellow stars). In the examples shown the naïve dissector contained one cell and the SNI dissector contained five.

Images are raw and unprocessed as grabbed directly from the confocal microscope. The sampling method used resulted in 10 sections being used from each animal. An example of the raw data gathered from one example from each group is shown in Table 1.

Table 1 shows the total cell counts from two individual animals, Naïve-1 (left) and SNI-1 (right). Q_i^- is the total number of microglial cell counts from all counting frames for an individual section (i = section number). A, B and C are the totals derived from the different multiplications of Q_i^- $(Q_i^- Q_i^-; Q_i^- Q_{i+1}^-; Q_i^- Q_{i+2}^-)$ used to complete the quadratic equation to estimate the coefficient of error.

Mean section thicknesses (t) were 29.3 μm (naïve-1) and 30.4 μm (SNI-1).

$$N = \sum Q^- \cdot \frac{1}{\text{tsf}} \cdot \frac{1}{\text{asf}} \cdot \frac{1}{\text{ssf}}$$
$$\text{Naïve-}\ 1 = 1181.717.1120 = 28634$$
$$\text{SNI-}\ 1 = 3941.657.1120 = 92444$$

The total number of cell counts per animal were: 116 ± 6 for naïve (n = 4) and 367 ± 28 for SNI (n = 4). Total microglial cell numbers (±SEM) as calculated above were; naïve: 28591 ± 1567; SNI: 82034 ± 5097 (Fig. 2a).

An important consideration in comparative stereological estimates is the individual estimates of total cell number. The group variability of cell number estimates is expressed by the coefficient of variation (CV = SD/mean). The observed variance in the estimates is the sum of the interanimal variability and the intraindividual variability as introduced by the precision of the stereological sampling procedure. The former is directly estimated from the data and the latter expressed by the coefficient of error (CE), defined as the ratio of SEM to the mean of the repeated estimates (West et al., 1991; Slomianka and West, 2005).

Two factors influence the CE of an estimate. Firstly, the variability of estimates made at the single section level, or ‘section noise’ denoted as V_{noise}—repeated systematic random sampling schemes within a single section will result in varying estimates of cell number. Secondly, the variability between sections; both in area and in cell density may vary throughout the volume of tissue being sampled. This is referred to as the variance due to systematic random sampling, V_{SRS}. The sum of these two variances gives the total variance of the estimate of N:

$$V_{\text{noise}} = \sum Q^{-}$$
$$V_{\text{SRS}} = \frac{3(A - V_{\text{noise}}) - 4B + C}{12}$$
$$\text{Total variance } (N) = V_{\text{noise}} + V_{\text{SRS}}$$
$$CE(\sum Q^{-}) = \frac{\sqrt{\text{Total variance}}}{\sum Q^{-}}$$

The biological variance of the group (CV) is determined by the formula: CV = SD/mean. Values for CV were: naïve = 0.06; SNI = 0.075. Values for CE were: naïve = 0.10; SNI = 0.07. The ratio of CE and observed variance of the group (CE^2/CV^2) was: Naïve = 0.35. SNI = 0.99.

Fig. 2b shows representative examples of sections from naïve (left) and SNI (right) spinal cords. In each case the central terminals of CTB-labelled sciatic nerve primary afferents are shown in red; IB4 labelling of non-peptidergic C-fibres in lamina II_{inner} shown in green and iba1 immunoreactive microglia shown in blue. The B subunit of cholera toxin (CTB) is a transganglionic tracer that binds specifically to the GM1 ganglioside on the surface of myelinated, but not unmyelinated, primary afferent fibers (Robertson and Grant, 1989). Injected into a peripheral nerve, it is taken up by myelinated primary afferents and transported to the dorsal root ganglia and on to their central terminals in the dorsal horn of the spinal cord (Robertson and Grant, 1985; Rivero-Melián and Grant, 1990, 1991; LaMotte et al., 1991; Rivero-Melián et al., 1992). CTB injection into the proximal stumps of the cut branches of the sciatic nerve in the SNI group selectively labeled the region of spinal cord innervated by the damaged nerves. For the naïve group the entire sciatic territory was labeled.

Bandeiraea simplicifolia isolectin B4 (IB4) binds to the non-peptidergic subpopulation of C-fibres that terminate in lamina II_{inner} of the dorsal horn (Wang et al., 1994). Following peripheral nerve injury this labeling transiently disappears resulting in a gap in labeling in the superficial dorsal horn (Molander et al., 1996). The labeling that persists represents the terminals of intact afferents. IB4 has also been described as a microglial marker (Wang et al., 1994). However, at the low concentrations and short incubation times used in these experiments it is selective for primary afferent terminals and no microglial labelling was seen.

Hindlimb nerve central projections to the spinal cord are somatotopically distributed. Fig. 3 shows a schematic longitudinal view of these projections to lamina II (Molander and Grant, 1986). Somatotopic maps to deeper laminae show a similar pattern (Molander and Grant, 1986; Woolf and Fitzgerald, 1986) although there is considerable individual variation (Molander and Grant, 1986). The sciatic nerve is composed of three main branches, the tibial, common peroneal and sural nerves. SNI involves transection of the tibial and common peroneal nerves (shown in red) while ‘sparing’ the sural nerve (shown in white). By mapping the CTB and IB4 labelling mediolaterally on the same section and rostrocaudally from serial sections taken throughout the lumbar cord it was possible to map the entire extent of the peripherally-lesioned primary afferent central projections and the intact

projections of adjacent nerves and, therefore, assess the somatotopic distribution of microglia in the spinal dorsal horn.

Fig. 4a shows the accuracy of this approach. In the naïve example (left), IB4 labeling is shown in green and CTB in red. The IB4 labeling was complete in the medio-lateral extent, the CTB only evident in the medial extent of the dorsal horn, the more lateral area in the image occupied by the central terminals of the adjacent, unlabeled saphenous nerve (shown in grey in Fig. 3). There was also clear delineation in the laminar distribution of the terminals, with CTB only labeling myelinated fibres terminating in deeper laminae, and the IB4 labeling restricted to lamina II_{inner} (Snider and McMahon, 1998). Following SNI, there was a clear gap in IB4 labeling, indicating the boundary of the central projections of the injured primary afferents. These afferents were directly labeled with CTB and there was a discrete delineation between the two, occupying adjacent and non-overlapping areas (boundary indicated by the white arrow).

Fig. 4b shows the microglial response to SNI. For clarity, IB4 is again shown in green with microglia shown in red (iba-1 immunoreactivity). In the naïve the IB4 label was again intact in the medio-lateral extent and there was sparse labelling of microglia. Following SNI there was the characteristic gap in IB4 labeling and the stereotypical microglial response with a marked increase in the number and density of cells. Interestingly, while the response was most evident around the terminal region of injured afferents, there was a clear spread laterally into the uninjured territory of the sural nerve. While generally widespread, the regions of densest microglial activation were observed in the more superficial laminae. Deeper laminae, despite receiving input from injured afferents show markedly reduced microglial activity.

Fig. 5 shows a reconstruction of the lumbar spinal cords from a naïve rat (top panel, left) and SNI rat (top panel, right). It is evident that there is a somatotopic distribution in microglial activation following SNI in that its extent is generally restricted to the central terminals of the cut nerves, as indicated by the CTB labelling. However, there is a small but distinct spread of microglia into the intact sural territory of the dorsal horn in L4/5 which can be clearly seen in the lower panel where the CTB and IB4 labelling (left) have been separated from the microglial labeling (right). However, the characteristic ‘saphenous notch’ (the gap in CTB labelling in L3 in both naïve and SNI where the adjacent saphenous nerve central terminals project)(Swett and Woolf, 1985) is also present in the microglial labeling in the SNI example. Therefore, there is a spread of microglial activity outside the injured central terminal fields following SNI, but it is restricted to the central terminals of the intact branch of the sciatic nerve. Directly adjacent, separate nerves, ie the saphenous, remain unaffected.

4. Discussion

4.1. Stereology

This study fulfills the requirements for estimating total microglial numbers in the spinal cord dorsal horn and represents the first attempt to do so. Previous studies The low CE^2/CV^2 indicates that most of the group variance of naïve animals reflects biological interanimal differences and not methodologically introduced variance. The higher CE^2/CV^2 value of the

SNI group may be a consequence of the low natural variance of that group ie, if there is little biological variance, then the counting precision will inevitably make a larger contribution to the group variance, despite the low CE. The lower biological variability of the SNI group may reflect a 'ceiling effect' of microglial activation/proliferation after peripheral nerve injury. In effect the dorsal horn becomes 'full' of microglia. Although the CE^2/CV^2 may indicate that much of the group variance in the SNI group originates from variance introduced by counting methodology, the low absolute value of the group variance and large experimental effect render it unnecessary to further improve estimate precision.

4.2. Somatotopy

The pattern of sensory input to the spinal cord is highly organised. The central projections of peripheral sensory nerves to lamina II of the dorsal horn are somatotopically arranged (Swett and Woolf, 1985; Molander and Grant, 1986; Woolf and Fitzgerald, 1986; Shortland et al., 1989) (Fig. 5). In addition, the projections of different fibre types within these nerves are discretely arranged in separate laminae (Snider and McMahon, 1998). However, the projections of peripheral nerves to lamina I show no clear somatotopy, with extensive overlap evident in both rostrocaudal and mediolateral extents (Molander and Grant, 1985, 1986). Previous studies examining somatotopic distribution of microglia after nerve injury have focussed on the infraorbital nerve and whisker follicle removal (Melzer et al., 1997). Within nucleus caudalis microglial activation was more exaggerated in superficial laminae, corresponding to C-fibre input - similar to the pattern seen in this study. It is an intriguing possibility that the microglial activation is driven by altered C-fibre input as a consequence of peripheral nerve injury as has been previously proposed (Mannion et al., 1996, 1998). Unmyelinated C-fibres have been shown to be more susceptible to peripheral nerve injury, with a large percentage of unmyelinated cells dying following peripheral nerve injury (Coggeshall et al., 1997) and further studies will be required to ascertain whether the microglial response is indicative of the first stage of degeneration of unmyelinated primary afferents following peripheral nerve injury.

The mediolateral spread of microglia outside the central terminal fields of the peripherally-injured hindlimb nerves may be of importance behaviorally. The skin region that is tested for reflex withdrawal thresholds following SNI is the receptive field area of the intact sural nerve (Decosterd and Woolf, 2000) ie that region of skin innervated by intact primary afferents whose central terminal fields are now occupied by activated microglia. Interestingly, the peripheral territory of the saphenous nerve remains normal in terms of cutaneous thresholds to mechanical stimulation after SNI (Decosterd and Woolf, 2000). The ability of activated microglia to affect neuronal excitability means that their presence in the sural territory of the dorsal horn is likely to have a profound influence on the function of second order neurons (Coull et al., 2005) and as such provides a potential mechanism for mechanical allodynia following SNI.

4.3. Concluding remarks

This study clearly shows the reproducibility of the optical fractionator and its suitability to providing estimates of total microglial cell number within the spinal cord dorsal horn and, therefore, provides a robust tool for future design-based and reliable quantitative studies.

Somatotopic mapping of the microglial response has revealed a previously undescribed spread of microglial proliferation outside the central territory of peripherally axotomised afferents and as such has major implications for the consequences of a pathological microglia response in ‘intact’ regions of the CNS.

References

Ayoub AE, Salm AK. Increased morphological diversity of microglia in the activated hypothalamic supraoptic nucleus. J Neurosci. 2003; 23(21):7759–7766. [PubMed: 12944504]

Coggeshall RE, Lekan HA, Doubell TP, Allchorne A, Woolf CJ. Central changes in primary afferent fibers following peripheral nerve lesions. Neuroscience. 1997; 77(4):1115–1122. [PubMed: 9130791]

Colburn RW, DeLeo JA, Rickman AJ, Yeager MP, Kwon P, Hickey WF. Dissociation of microglial activation and neuropathic pain behaviors following peripheral nerve injury in the rat. J Neuroimmunol. 1997; 79(2):163–175. [PubMed: 9394789]

Colburn RW, Rickman AJ, DeLeo JA. The effect of site and type of nerve injury on spinal glial activation and neuropathic pain behavior. Exp Neurol. 1999; 157(2):289–304. [PubMed: 10364441]

Coull JA, Beggs S, Boudreau D, Boivin D, Tsuda M, Inoue K, Gravel C, Salter MW, De Koninck Y. BDNF from microglia causes the shift in neuronal anion gradient underlying neuropathic pain. Nature. 2005; 438(7070):1017–1021. [PubMed: 16355225]

Coyle DE. Partial peripheral nerve injury lead to activation of astroglia and microglia which parallels the development of allodynic behavior. Glia. 1998; 23:75–83. [PubMed: 9562186]

Decosterd I, Woolf CJ. Spared nerve injury: an animal model of persistent peripheral neuropathic pain. Pain. 2000; 87(2):149–158. [PubMed: 10924808]

Eriksson NP, Persson JK, Svensson M, Arvidsson J, Molander C, Aldskogius H. A quantitative analysis of the microglial cell reaction in central primary sensory projection territories following peripheral nerve injury in the adult rat. Exp Brain Res. 1993; 96(1):19–27. [PubMed: 8243580]

Fu KY, Light AR, Matsushima GK, Maixner W. Microglial reactions after subcutaneous formalin injection into the rat hind paw. Brain Res. 1999; 825(1–2):59–67. [PubMed: 10216173]

Gehrmann J, Monaco S, Kreutzberg SW. Spinal cord microglial cells and DRG satellite cells rapidly respond to transection of the rat sciatic nerve. Restor Neurol Neurosci. 1991; 2:181–198. [PubMed: 21551602]

Herzberg U, Sagen J. Peripheral nerve exposure to HIV viral envelope protein gp120 induces neuropathic pain and spinal gliosis. J Neuroimmunol. 2001; 116:29–39. [PubMed: 11311327]

Ji RR, Kohno T, Moore KA, Woolf CJ. Central sensitization and LTP: do pain and memory share similar mechanisms? Trends Neurosci. 2003; 26(12):696–705. [PubMed: 14624855]

Jin SX, Zhuang ZY, Woolf CJ, Ji RR. p38 mitogen-activated protein kinase is activated after a spinal nerve ligation in spinal cord microglia and dorsal root ganglion neurons and contributes to the generation of neuropathic pain. J Neurosci. 2003; 23(10):4017–4022. [PubMed: 12764087]

Kreutzberg GW. Microglia: a sensor for pathological events in the CNS. Trends Neurosci. 1996; 19(8): 312–318. [PubMed: 8843599]

LaMotte CC, Kapadia SE, Shapiro CM. Central projections of the sciatic, saphenous, median, and ulnar nerves of the rat demonstrated by transganglionic transport of choleragenoid-HRP (B-HRP) and wheat germ agglutinin-HRP (WGA-HRP). J Comp Neurol. 1991; 311:546–562. [PubMed: 1721924]

Liu L, Tornqvist E, Mattsson P, Eriksson NP, Persson JK, Morgan BP, Aldskogius H, Svensson M. Complement and clusterin in the spinal cord dorsal horn and gracile nucleus following sciatic nerve injury in the adult rat. Neuroscience. 1995; 68(1):167–179. [PubMed: 7477922]

Long JM, Kalehua AN, Muth NJ, Hengemihle J, Mouton PR. Stereological estimation of total microglia number in mouse hippocampus. J Neurosci Methods. 1998; 84(1–2):101–108. [PubMed: 9821640]

Mannion RJ, Doubell TP, Coggeshall RE, Woolf CJ. Collateral sprouting of uninjured primary afferent A-fibers into the superficial dorsal horn of the adult rat spinal cord after topical capsaicin treatment to the sciatic nerve. J Neurosci. 1996; 16(16):5189–5195. [PubMed: 8756447]

Mannion RJ, Doubell TP, Gill H, Woolf CJ. Deafferentation is insufficient to induce sprouting of A-fibre central terminals in the rat dorsal horn. J Comp Neurol. 1998; 393(2):135–144. [PubMed: 9548693]

Melzer P, Zhang MZ, McKanna JA. Infraorbital nerve transection and whisker follicle removal in adult rats affect microglia and astrocytes in the trigeminal brainstem. A study with lipocortin1- and S100beta-immunohistochemistry. Neuroscience. 1997; 80(2):459–472. [PubMed: 9284349]

Moalem G, Tracey DJ. Immune and inflammatory mechanisms in neuropathic pain. Brain Res Brain Res Rev. 2006; 51(2):240–264.

Molander C, Grant G. Cutaneous projections from the rat hindlimb foot to the substantia gelatinosa of the spinal cord studied by transganglionic transport of WGA-HRP conjugate. J Comp Neurol. 1985; 237(4):476–484. [PubMed: 2413084]

Molander C, Grant G. Laminar distribution and somatotopic organization of primary afferent fibers from hindlimb nerves in the dorsal horn. A study by transganglionic transport of horseradish peroxidase in the rat. Neuroscience. 1986; 19(1):297–312. [PubMed: 3785668]

Molander C, Wang HF, Rivero-Melián C, Grant G. Early decline and late restoration of spinal cord binding and transganglionic transport of isolectin B4 from Griffonia simplicifolia I after peripheral nerve transection or crush. Restor Neurol Neurosci. 1996; 10:123–133. [PubMed: 21551513]

Nakajima K, Kohsaka S. Microglia: activation and their significance in the central nervous system. J Biochem (Tokyo). 2001; 130:169–175. [PubMed: 11481032]

Perry VH. Modulation of microglia phenotype. Neuropathol Appl Neurobiol. 1994; 20:177.

Rivero-Melián C, Grant G. Distribution of lumbar dorsal root fibers in the lower thoracic and lumbosacral spinal cord of the rat studied with choleragenoid horseradish peroxidase conjugate. J Comp Neurol. 1990; 299:470–481. [PubMed: 2243162]

Rivero-Melián C, Grant G. Choleragenoid horseradish peroxidase used for studying projections of some hindlimb cutaneous nerves and plantar foot afferents to the dorsal horn and Clarke's column in the rat. Exp Brain Res. 1991; 84:125–132. [PubMed: 1713167]

Rivero-Melián C, Rosario C, Grant G. Demonstration of transganglionically transported choleragenoid in rat spinal cord by immunofluorescence cytochemistry. Neurosci Lett. 1992; 145:114–117. [PubMed: 1281298]

Robertson B, Grant G. A comparison between wheatgerm agglutinin and choleragenoid-horseradish peroxidase as anterogradely transported markers in central branches of primary sensory neurones in the rat with some observations in the cat. Neuroscience. 1985; 14:895–905. [PubMed: 3838806]

Robertson B, Grant G. Immunocytochemical evidence for the localization of the GM1 ganglioside in carbonic anhydrase-containing and RT 97-immunoreactive rat primary sensory neurons. J Neurocytol. 1989; 18:77–86. [PubMed: 2496205]

Salter MW. Cellular signalling pathways of spinal pain neuroplasticity as targets for analgesic development. Curr Top Med Chem. 2005; 5(6):557–567. [PubMed: 16022678]

Scholz J, Woolf CJ. Can we conquer pain? Nat Neurosci. 2002; 5(Suppl):1062–1067. [PubMed: 12403987]

Shortland P, Woolf CJ, Fitzgerald M. Morphology and somatotopic organization of the central terminals of hindlimb hair follicle afferents in the rat lumbar spinal cord. J Comp Neurol. 1989; 289(3):416–433. [PubMed: 2808777]

Slomianka L, West MJ. Estimators of the precision of stereological estimates: an example based on the CA1 pyramidal cell layer of rats. Neuroscience. 2005; 136(3):757–767. [PubMed: 16344149]

Snider WD, McMahon SB. Tackling pain at the source: new ideas about nociceptors. Neuron. 1998; 20(4):629–632. [PubMed: 9581756]

Stoll G, Jander S. The role of microglia and macrophages in the pathophysiology of the CNS. Prog Neurobiol. 1999; 58:233–247. [PubMed: 10341362]

Streit WJ, Graeber MB, Kreutzberg GW. Functional plasticity of microglia: a review. Glia. 1988; 1(5): 301–307. [PubMed: 2976393]

Swett JE, Woolf CJ. The somatotopic organization of primary afferent terminals in the superficial laminae of the dorsal horn of the rat spinal cord. J Comp Neurol. 1985; 231(1):66–77. [PubMed: 3968229]

Tsuda M, Shigemoto-Mogami Y, Koizumi S, Mizokoshi A, Kohsaka S, Salter MW, Inoue K. P2X4 receptors induced in spinal microglia gate tactile allodynia after nerve injury. Nature. 2003; 424(6950):778–783. [PubMed: 12917686]

Tsuda M, Inoue K, Salter MW. Neuropathic pain and spinal microglia: a big problem from molecules in “small” glia. Trends Neurosci. 2005; 28(2):101–107. [PubMed: 15667933]

Wang H, Rivero-Melián C, Robertson B, Grant G. Transganglionic transport and binding of the isolectin B4 from Griffonia simplicifolia I in rat primary sensory neurons. Neuroscience. 1994; 62:539– 551. [PubMed: 7530347]

Watkins LR, Milligan ED, Maier SF. Glial activation: a driving force for pathological pain. Trends Neurosci. 2001; 24(8):450–455. [PubMed: 11476884]

West MJ, Slomianka L, Gundersen HJ. Unbiased stereological estimation of the total number of neurons in the subdivisions of the rat hippocampus using the optical fractionator. Anat Rec. 1991; 231(4):482–497. [PubMed: 1793176]

West MJ, Ostergaard K, Andreassen OA, Finsen B. Estimation of the number of somatostatin neurons in the striatum: an in situ hybridization study using the optical fractionator method. J Comp Neurol. 1996; 370(1):11–22. [PubMed: 8797153]

Wieseler-Frank J, Maier SF, Watkins LR. Activation and pathological pain. Neurochem Int. 2004; 45(2–3):389–395. [PubMed: 15145553]

Wirenfeldt M, Dalmau I, Finsen B. Estimation of absolute microglial cell numbers in mouse fascia dentata using unbiased and efficient stereological cell counting principles. Glia. 2003; 44(2):129–139. [PubMed: 14515329]

Woolf CJ, Fitzgerald M. Somatotopic organization of cutaneous afferent terminals and dorsal horn neuronal receptive fields in the superficial and deep laminae of the rat lumbar spinal cord. J Comp Neurol. 1986; 251(4):517–531. [PubMed: 3782502]

Zhang J, De Koninck Y. Spatial and temporal relationship between monocyte chemoattractant protein-1 expression and spinal glial activation following peripheral nerve injury. J Neurochem. 2006; 97(3):772–783. [PubMed: 16524371]

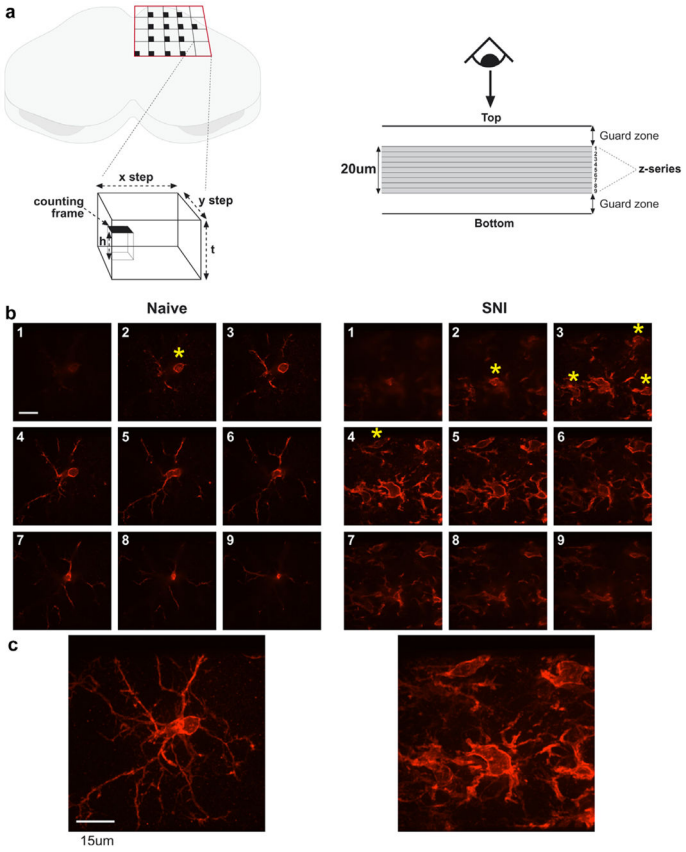

Fig. 1.

Schematic showing the sampling paradigm for the stereological analysis of microglia within the dorsal horn (a). Examples of images within optical dissectors for naïve and SNI rats are shown in (b). Extended focus images of each full z-series are shown in (C). Yellow asterisks indicate the emergence of a soma coming into focus to be counted. Scale bar = 15 μm. (For interpretation of the references to color in this figure legend, the reader is referred to the web version of this paper.)

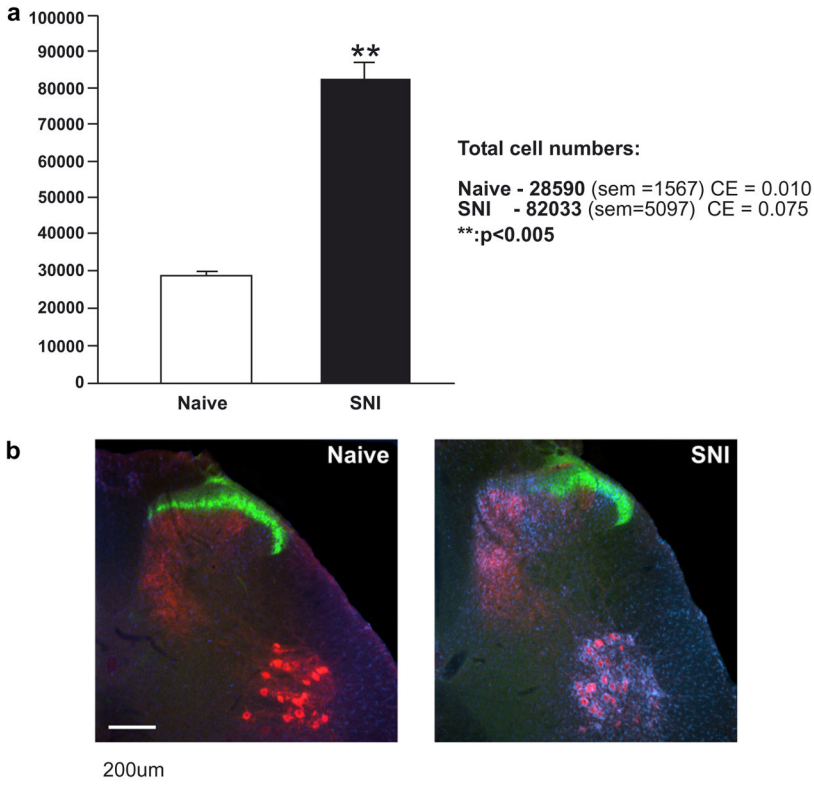

Fig. 2.

Quantitative analysis of microglia in the dorsal horn of naïve and SNI rats (a). Following SNI there is a marked significant increase in the ipsilateral dorsal horn ($p < 0.005$). (b) Examples of naïve and SNI sections showing the characteristic microglial response (blue). CTB-labelled central terminals are shown in red and IB4 labelling in green. Scale bar = 200 μm. (For interpretation of the references to color in this figure legend, the reader is referred to the web version of this paper.)

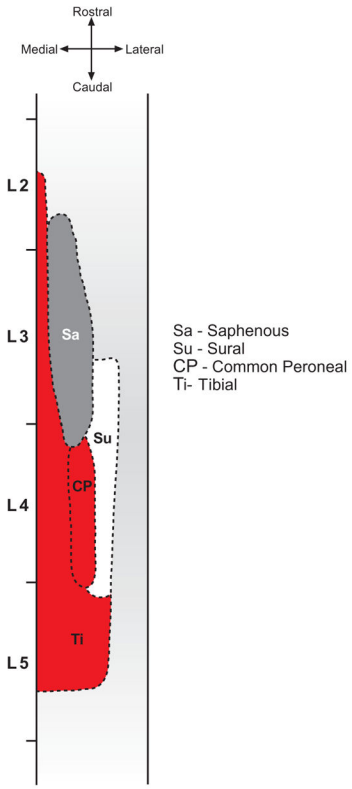

Fig. 3.

Somatotopic dorsal view illustration of the central terminal fields of indicated hindlimb nerves in lamina II of the spinal cord (adapted from Molander and Grant, 1986, with permission).

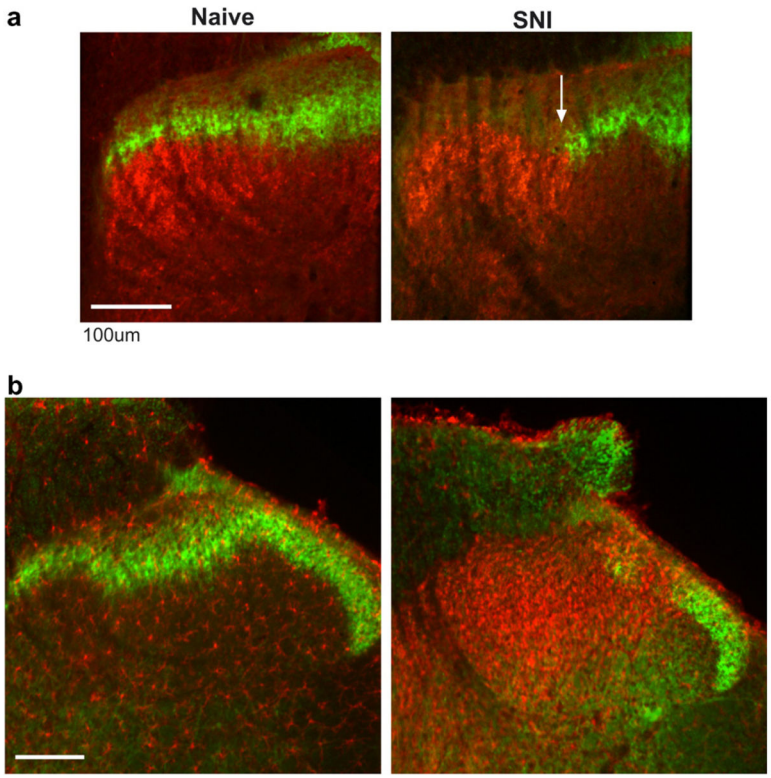

Fig. 4.

(a) Labelling of injured primary afferents with CTB (red) and uninjured terminals with IB4 (green). Following SNI (right) there is a clear delineation between the terminal fields of the two groups of afferents (white arrow). (b) Spread of microglia (red) out of the terminal fields of injured primary afferents and into the more lateral, uninjured, sural territory. Scale bar = 100 μm. (For interpretation of the references to color in this figure legend, the reader is referred to the web version of this paper.)

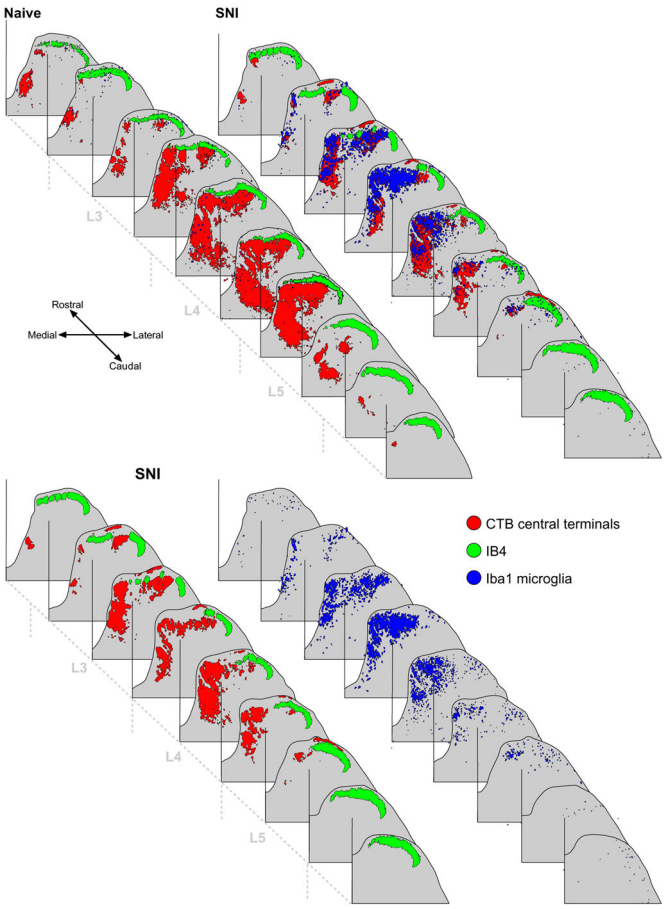

Fig. 5.

Top panel: Reconstructions of naïve and SNI lumbar dorsal horns showing the somatotopic nature of the microglial response to PNI. Microglia are indicated in blue, CTB in red and IB4 in green. Bottom panel: SNI dorsal horn with the microglial labelling (right) separated from the primary afferent labelling (left). While the majority of microglial activity is restricted to the injured central terminal fields, shown by overlap of the blue and red labelling, there is a small but distinct spread of microglial labelling into the intact sural territory. (For interpretation of the references to color in this figure legend, the reader is referred to the web version of this paper.)

Table 1

Calculation of total iba-1ir microglial cell numbers

Naïve-1					**SNI-1**				
Section	Q_i^-	$Q_i^- \cdot Q_i^-$	$Q_i^- \cdot Q_{i+1}^-$	$Q_i^- \cdot Q_{i+2}^-$	**Section**	Q_i^-	$Q_i^- \cdot Q_i^-$	$Q_i^- \cdot Q_{i+1}^-$	$Q_i^- \cdot Q_{i+2}^-$
1	7	49	70	70	1	13	169	546	377
2	10	100	100	180	2	42	1764	1218	1260
3	10	100	180	150	3	29	841	870	1218
4	18	324	270	216	4	30	900	1260	2010
5	15	225	180	150	5	42	1764	2814	1470
6	12	144	120	60	6	67	4489	2345	3819
7	10	100	50	160	7	35	1225	1995	1505
8	5	25	80	75	8	57	3249	2451	2052
9	16	256	240	0	9	43	1849	1548	0
10	15	225	0	0	10	36	1296	0	0
ΣQ^-	118	1548	1290	1061	ΣQ	394	17546	15047	13711
		A	*B*	*C*			*A*	*B*	*C*